

A POTENTIAL MODEL REPRESENTATION OF TWO-NUCLEON DATA BELOW 315 MeV

T HAMADA† and I D JOHNSTON

The Daily Telegraph Theoretical Department, School of Physics ††, University of Sydney, Sydney, N S W, Australia

Received 14 November 1961

Abstract: An energy independent nucleon-nucleon potential model is described. The model represents the two-nucleon data below 315 MeV more faithfully than any other potential model known to date. The data include the effective range expansion parameters and the deuteron properties as well as the scattering data at higher energies. It is of special significance that the n-p data have been represented by the energy independent potential model in a satisfactory manner for the first time. For this purpose a quadratic *LS* potential was found essential in the $T = 0$ state. The $T = 1$ potential differs little from those previously proposed by several authors. The phase shifts predicted by the model are in fair agreement with the solutions YLAM ($T = 1$) and YLAN3M ($T = 0$) recently found by the Yale group.

1. Introduction

One of the present authors recently reported on a potential model which can represent the two-nucleon data in the non-relativistic region reasonably well^{1, 2)}. The $T = 1$ potential, referred to as H1 potential in the following, is not qualitatively different from those proposed earlier by several authors³. The fits to the p-p data are remarkably good considering the wide energy range covered in the work. The Yale group has since published results⁴⁾ of a phase shift analysis of p-p scattering from 9.7 to 345 MeV. Comparison of the phase shifts predicted by the H1 potential with the best solution YLAM indicated that slight modification of the H1 potential could improve the fit still further. In the present paper the new version of the $T = 1$ potential thus obtained is described and its predictions are compared in full detail with the experimental data.

The situation is much less satisfactory about the $T = 0$ potential²⁾, referred to as H0 potential in the present paper. The potential is not strictly energy independent and the fits to the n-p data are somewhat poorer even though the uncertainties in the data are rather large. It was pointed out that a weak but long ranged quadratic *LS* potential is necessary in order to make the 3D_2 phase shift small at higher energies. A possible improvement in the form of the

† Address after January, 1962: Dept. of Physics, Ibaraki University, Mito, Japan.

†† Also supported by the Nuclear Research Foundation within the University of Sydney.

‡ For a brief review on this subject the reader is referred to Noyes' paper presented at the 1960 Rochester conference³⁾.

quadratic LS potential employed in H0 has already been suggested (sect 2 of ref ²) Comparison with the recent results of the n-p phase shift analysis by the Yale group ⁵) confirmed the idea and a new independent $T = 0$ potential has been constructed accordingly This new $T = 0$ potential and its predictions of deuteron properties and n-p scattering, when combined with the new version of the $T = 1$ potential, are described in the present paper

It will be shown that our new potential model represents the two-nucleon data in the non-relativistic region more faithfully than any other models proposed to date To our knowledge this is the first time both p-p and n-p data have been consistently represented by an energy independent potential model We believe that our model may be used in the calculation of nuclear systems containing more than two nucleons We also believe that the model is useful in checking the compatibility of any potentials, derived field theoretically or otherwise, with the experimental two-nucleon data

2. Potential Model

Our model consists of four terms

$$V = V_C + V_T S_{12} + V_{LS}(\mathbf{L} \cdot \mathbf{s}) + V_{LL} L_{12}, \quad (1)$$

where C, T, LS and LL refer to central, tensor, linear LS and quadratic LS potential, respectively, and L_{12} is the operator defined by

$$\begin{aligned} L_{12} &= (\sigma_1 \cdot \sigma_2) \mathbf{L}^2 - \frac{1}{2} \{ (\sigma_1 \cdot \mathbf{L})(\sigma_2 \cdot \mathbf{L}) + (\sigma_2 \cdot \mathbf{L})(\sigma_1 \cdot \mathbf{L}) \} \\ &= \{ \delta_{LJ} + (\sigma_1 \cdot \sigma_2) \} \mathbf{L}^2 - (\mathbf{L} \cdot \mathbf{s})^2, \end{aligned} \quad (2)$$

and constitutes a major difference between the present model and H0 or H1

The V_i ($i = C, T, LS, LL$) are allowed to be spin-parity dependent. They are given by

$$\begin{aligned} V_C &= 0.08 \left(\frac{1}{3} \mu \right) (\mathbf{r}_1 \cdot \mathbf{r}_2) (\sigma_1 \cdot \sigma_2) Y(x) \cdot [1 + a_C Y(x) + b_C Y^2(x)], \\ V_T &= 0.08 \left(\frac{1}{3} \mu \right) (\mathbf{r}_1 \cdot \mathbf{r}_2) Z(x) \cdot [1 + a_T Y(x) + b_T Y^2(x)], \\ V_{LS} &= \mu G_{LS} Y^2(x) [1 + b_{LS} Y(x)], \\ V_{LL} &= \mu G_{LL} x^{-2} Z(x) [1 + a_{LL} Y(x) + b_{LL} Y^2(x)], \end{aligned} \quad (3)$$

where μ is the pion mass [†], x the inter-nucleon distance measured in μ^{-1} and

$$Y(x) = e^{-x}/x, \quad Z(x) = (1 + 3/x + 3/x^2) Y(x).$$

For sufficiently large x , V_C and V_T reduce to the well-known one-pion-exchange potential (OPEP) with the equivalent pseudo-vector coupling constant 0.08 The coefficients a_C , b_C , a_T and b_T determine the deviation of

[†] The values $\mu = 139.4 = (1.415 \text{ fm})^{-1}$ and $M/\mu = 6.73$ (M is the nucleon mass) have been used in the numerical calculations

the potentials from OPEP at smaller x , and V_{LS} represents a short range linear LS potential whose strength G_{LS} depends on the parity of the state concerned. The special functional form of V_{LL} has been taken from available pion theory calculations^{6,7)} Its strength G_{LL} , particularly its sign, was determined phenomenologically.

The presence of hard cores in all states has been assumed. At earlier stages of the search for the potential, the hard core radius was allowed to be spin-parity dependent. It turned out, however, that the hard core radius could be made the same in all states without much difficulty. There is no theoretical reason why the hard core, if ever present, should have the same radius in all states, yet, the same hard core radius would make the application of the present model to systems of more than two nucleons considerably simpler[†]. The hard core radius is thus

$$x_0 = 0.343 \text{ (all states)} \quad (4)$$

Other parameters in (3) are given in table 1. Eqs. (1) to (4) together with table 1 define our potential model. The potentials are plotted in figs. 1 to 3.

TABLE 1
Numerical values of the parameters in (3)

state	a_C	b_C	a_T	b_T	G_{LS}	b_{LS}	G_{LL}	a_{LL}	b_{LL}
singlet even	+8.7	+10.6					-0.000891	+0.2	-0.2
triplet odd	-9.07	+3.48	-1.29	+0.55	+0.1961	-7.12	-0.000891	-7.26	+6.92
triplet even	+6.0	-1.0	-0.5	+0.2	+0.0743	-0.1	+0.00267	+1.8	-0.4
singlet odd	-8.0	+12.0					-0.00267	+2.0	+6.0

Hard core radius $x_0 = 0.343$ in all states

For later references we give here the Schrodinger equations when the potential is given by (1). Writing

$$\kappa^2 = ME_{\text{cm}}/\mu^2, \quad U_i(x) = (M/\mu^2)V_i(x),$$

they read
singlet

$$\{d^2/dx^2 + \kappa^2 - J(J+1)/x^2 - U_C(x) + 2J(J+1)U_{LL}(x)\}u(x) = 0, \quad (5)$$

triplet $L = J$

$$\begin{aligned} \{d^2/dx^2 + \kappa^2 - J(J+1)/x^2 - U_C(x) - 2U_T(x) + U_{LS}(x) \\ - [2J(J+1) - 1]U_{LL}(x)\}v_J(x) = 0, \end{aligned} \quad (6)$$

[†] We are grateful to Professor J. M. Blatt for some conversations on this subject.

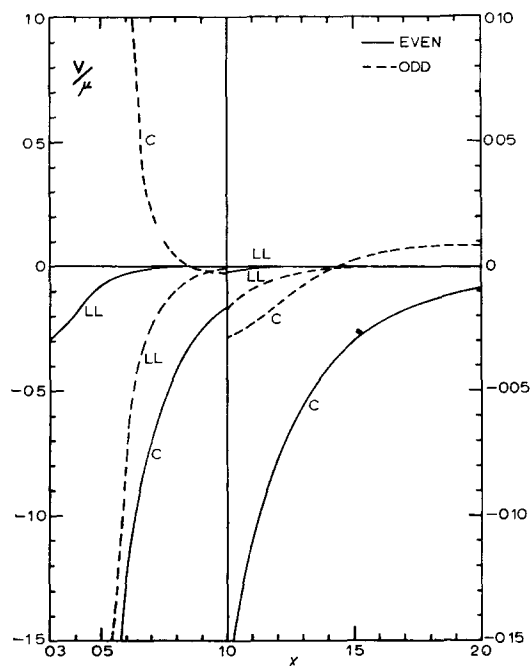


Fig 1 The potential model in the singlet states defined by eqs (1) to (4) and table 1

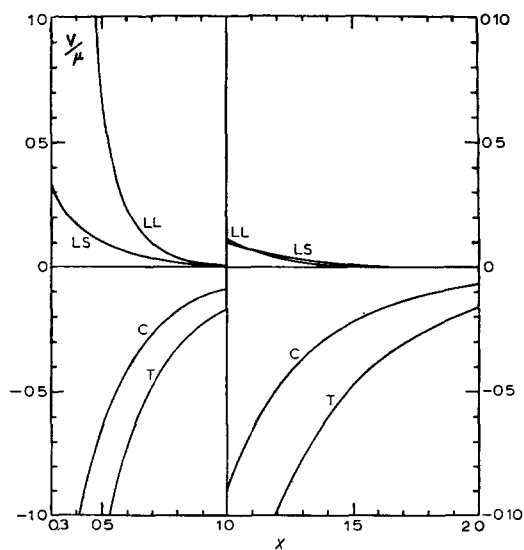


Fig 2 The triplet even parity potential defined by eqs (1) to (4) and table 1.

triplet $L = J \pm 1$:

$$\begin{aligned}
 &\{d^2/dx^2 + \kappa^2 - J(J-1)/x^2 - U_C(x) + 2(J-1)/(2J+1)U_T(x) \\
 &\quad - (J-1)U_{LS}(x) - (J-1)U_{LL}(x)\}u_J(x) \\
 &\quad - 6\sqrt{J(J+1)}/(2J+1)U_T(x)w_J(x) = 0, \\
 &\{d^2/dx^2 + \kappa^2 - (J+1)(J+2)/x^2 - U_C(x) \\
 &\quad + 2(J+2)/(2J+1)U_T(x) + (J+2)U_{LS}(x) \\
 &\quad + (J+2)U_{LL}(x)\}w_J(x) - 6\sqrt{J(J+1)}/(2J+1)U_T(x)u_J(x) = 0
 \end{aligned} \tag{7}$$

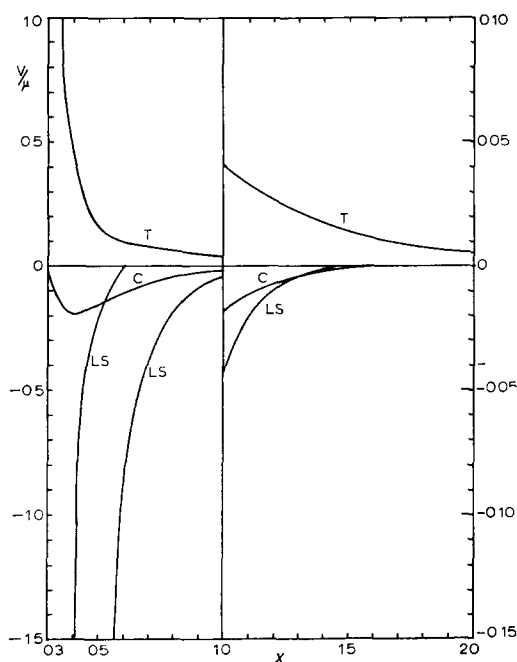


Fig 3 The triplet odd parity potential defined by eqs (1) to (4) and table 1

We note that the quadratic LS potential is more important in the uncoupled states (singlet and triplet $L = J$ states) than in the coupled states. For the coupled states the introduction of V_{LL} is equivalent to changing V_{LS} into $V_{LS} + V_{LL}$.

3. Deuteron Problem and Effective Range Expansion Parameters

Our triplet even parity potential predicts the following deuteron data

binding energy	$\varepsilon = 2.226 \text{ MeV},$	
electric quadrupole moment	$Q = 2.85 \times 10^{-27} \text{ cm}^2,$	
effective range	$\rho(-\varepsilon, -\varepsilon) = 1.77 \text{ fm},$	(8)
D-state probability	$P_D = 6.97 \%,$	
asymptotic D to S wave ratio	$A_D/A_S = 0.02656$	

The contribution to the deuteron magnetic moment from the V_{LS} and V_{LL} is about $+0.003$ nuclear magneton. This is only 13 % of the observed difference $\mu_n + \mu_p - \mu_d = +0.0225$ n.m. so that no new difficulty is met in this respect. It is concluded that the deuteron data are represented in satisfactory manner by our model. The deuteron wave function is given in table 2.

TABLE 2
The deuteron wave function

x	$u(x)$	$w(x)$	x	$u(x)$	$w(x)$
0.4	0.1096	0.0621	3.2	0.3484	0.0555
0.5	0.2718	0.1412	3.4	0.3267	0.0491
0.6	0.3891	0.1856	3.6	0.3062	0.0435
0.7	0.4697	0.2083	3.8	0.2869	0.0387
0.8	0.5229	0.2178	4.0	0.2688	0.0345
0.9	0.5564	0.2189	4.2	0.2519	0.0308
1.0	0.5757	0.2149	4.4	0.2359	0.0276
1.1	0.5849	0.2077	4.6	0.2210	0.0247
1.2	0.5870	0.1987	4.8	0.2070	0.0222
1.3	0.5839	0.1888	5.0	0.1939	0.0200
1.4	0.5771	0.1784	5.2	0.1816	0.0181
1.5	0.5678	0.1680	5.4	0.1701	0.0163
1.6	0.5568	0.1578	5.6	0.1593	0.0148
1.7	0.5445	0.1479	5.8	0.1492	0.0134
1.8	0.5313	0.1385	6.0	0.1397	0.0122
1.9	0.5177	0.1297	6.5	0.1186	0.0096
2.0	0.5038	0.1213	7.0	0.1007	0.0077
2.1	0.4898	0.1134	7.5	0.0854	0.0062
2.2	0.4758	0.1061	8.0	0.0725	0.0050
2.3	0.4619	0.0992	8.5	0.0615	0.0040
2.4	0.4482	0.0929	9.0	0.0522	0.0033
2.5	0.4347	0.0869	9.5	0.0443	0.0027
2.6	0.4214	0.0814	10.0	0.0376	0.0022
2.7	0.4085	0.0763			
2.8	0.3958	0.0715			
2.9	0.3835	0.0670			
3.0	0.3715	0.0629			

Entries are the radial S and D wave functions (multiplied by x) calculated from the potential defined by eqs (1) to (4) and table 1. They are normalized to $\int_{x_0}^{\infty} (u^2 + w^2) dx = 0.9000$ with $x_0 = 0.343$. See ref. ⁸⁾ for the deuteron properties derived from this wave function.

It may be appropriate here to indicate briefly the effects of V_{LS} and V_{LL} on the deuteron properties. Since both V_{LS} and V_{LL} vanish in the predominant S state, one expects that they will be relatively unimportant. If one puts $V_{LS} = 0$ in our triplet even parity potential, the hard core radius x_0 has to be reduced by 0.003 to 0.340 in order to reproduce the correct binding energy. The effective range $\rho(-\epsilon, -\epsilon)$ is still 1.77 fm, but Q and P_D are now 2.82×10^{-27} cm² and 6.77 %, respectively. If, on the other hand, one puts $V_{LL} = 0$ (keeping V_{LS}), $x_0 = 0.329$, $\rho(-\epsilon, -\epsilon) = 1.77$ fm, $Q = 2.81 \times 10^{-27}$ cm² and

$P_D = 6.44\%$. Thus V_{LS} and V_{LL} are indeed unimportant as far as the deuteron problem is concerned, unless they are unreasonably strong.

The effective range expansion for the 1S_0 phase shift in the n-p scattering reads

$$k \cot \delta(^1S_0) = -\frac{1}{^1a} + \frac{1}{2} {}^1r_e k^2 - P {}^1r_e {}^3k^4 + \dots \quad (9)$$

Our singlet even parity potential gives

$$^1a = -17.0 \text{ fm}, \quad {}^1r_e = 2.83 \text{ fm}, \quad P = +0.016. \quad (10)$$

Notice that our model predicts ^{8,9)} a positive shape parameter P in spite of its large hard core radius $x_0 = 0.343 = 0.485 \text{ fm}$.

The n-p scattering length 1a in (10) is higher than the experimental value of -23.7 fm by 6.7 fm . It is, on the other hand, in good agreement with the p-p scattering length † , $-17 \pm 3 \text{ fm}$. This is the manifestation of the well-known apparent violation of charge independence in the 1S_0 state. We have neglected this effect by assuming strict charge independence. It seems natural, then, to choose the potential model which represents the p-p scattering more faithfully, since at low energies the 1S_0 scattering is relatively more important in the p-p scattering (pure 1S_0) than in the n-p scattering (1S_0 and 3S_1). We only mention here that, with the same values of a_c and b_c as given in table 1, the scattering length 1a could be made -23.7 fm by reducing x_0 by 0.002 . The effective range would then be 2.73 fm .

4. p-p Scattering

The $T = 1$ phase shifts calculated from the model are shown in tables 3 and 4(a). All these phase shifts have been calculated from the nuclear potential alone so that they are, rigorously speaking, the n-p phase shifts. The difference between the n-p and the nuclear p-p phase shifts should be negligible in the energy region we are concerned with in this section. For coupled partial waves the parametrization of the scattering matrix is that of Blatt and Biedenharn ¹¹⁾. In the phase shift analyses of experimental data, the parametrization in the nuclear bar scheme has been used extensively ^{4,12)}. We have, therefore, also shown the coupled phase shifts in the nuclear bar scheme in table 4(b).

The singlet even parity phase shifts shown in table 3 are in good agreement ⁴⁾ with YLAM. Our $\delta(^1S_0)$ is higher than YLAM by 0.02 to 0.05 rad for $E < 180 \text{ MeV}$ but almost identical to YLAM above 200 MeV . The $\delta(^1D_2)$ runs below YLAM for $E < 180 \text{ MeV}$ and above YLAM for higher energies. The discrepancy is, however, well within the standard deviation of YLAM.

[†] By this we mean the p-p scattering length when the Coulomb potential is switched off. See, for example, Bethe and Morrison ¹⁰⁾.

TABLE 3

Singlet even parity nuclear phase shifts calculated from the potential defined by eqs (1) to (4) and table 1

E (MeV)	1S_0	1D_2	1G_4	1I_6
10	0 991	0 003		
20	0 890	0 010		
40	0 734	0 024	0 002	
60	0 614	0 038	0 004	0 001
80	0 515	0 053	0 005	0 001
100	0 429	0 067	0 007	0 002
120	0 353	0 082	0 009	0 002
140	0 283	0 095	0 011	0 003
160	0 220	0 108	0 013	0 003
180	0 161	0 121	0 014	0 004
200	0 106	0 134	0 016	0 004
220	0 053	0 145	0 017	0 005
240	0 004	0 157	0 019	0 005
260	-0 043	0 167	0 020	0 006
280	-0 087	0 177	0 022	0 006
300	-0 130	0 186	0 023	0 006
320	-0 171	0 194	0 024	0 007

TABLE 4 (a)

Triplet odd parity nuclear Blatt-Biedenharn phase shifts, calculated from the potential defined by eqs (1) to (4) and table 1

E (MeV)	3P_0	3P_1	3F_3	3H_3	3P_2	3F_2	ϵ_1	3F_4	3H_4	ϵ_4	3H_6	3K_6	ϵ_6
10	0 069	-0 038	-0 001		0 012	-0 001	-0 316						
20	0 127	-0 079	-0 003		0 032	-0 002	-0 332	0 001	-0 000	-0 736			
40	0 182	-0 125	-0 009	-0 001	0 081	-0 003	-0 310	0 003	-0 002	-0 735			
60	0 188	-0 166	-0 015	-0 002	0 128	-0 001	-0 282	0 006	-0 004	-0 731	0 001	-0 001	-0 760
80	0 171	-0 199	-0 021	-0 004	0 172	0 002	-0 255	0 010	-0 005	-0 721	0 002	-0 001	-0 766
100	0 145	-0 230	-0 026	-0 005	0 208	0 006	-0 233	0 014	-0 006	-0 708	0 003	-0 002	-0 772
120	0 114	-0 258	-0 031	-0 007	0 239	0 010	-0 213	0 018	-0 007	-0 690	0 004	-0 002	-0 779
140	0 079	-0 284	-0 036	-0 008	0 264	0 013	-0 197	0 022	-0 007	-0 668	0 005	-0 003	-0 785
160	0 044	-0 309	-0 040	-0 010	0 284	0 016	-0 182	0 027	-0 006	-0 641	0 006	-0 004	-0 790
180	0 009	-0 333	-0 044	-0 011	0 299	0 018	-0 169	0 032	-0 006	-0 613	0 007	-0 004	-0 795
200	-0 026	-0 357	-0 048	-0 013	0 308	0 019	-0 160	0 038	-0 005	-0 580	0 008	-0 005	-0 799
220	-0 060	-0 380	-0 052	-0 014	0 315	0 020	-0 146	0 044	-0 004	-0 544	0 009	-0 005	-0 802
240	-0 094	-0 402	-0 056	-0 015	0 319	0 019	-0 137	0 051	-0 003	-0 508	0 010	-0 006	-0 804
260	-0 127	-0 423	-0 059	-0 016	0 320	0 019	-0 128	0 058	-0 001	-0 471	0 011	-0 006	-0 806
280	-0 159	-0 443	-0 063	-0 017	0 319	0 017	-0 119	0 066	0 001	-0 435	0 013	-0 006	-0 806
300	-0 191	-0 464	-0 066	-0 019	0 316	0 015	-0 112	0 075	0 002	-0 397	0 014	-0 007	-0 806
320	-0 222	-0 484	-0 070	-0 020	0 311	0 013	-0 106	0 085	0 004	-0 358	0 015	-0 007	-0 804

The same phase shifts for coupled partial waves in the nuclear bar scheme are shown in table 4(b)

For $\delta(^1G_4)$ the agreement is even better. The agreement is complete below ≈ 120 MeV, above which energy our $\delta(^1G_4)$ runs above YLAM. The difference increases with energy but does not exceed 0.008.

The good overall agreement of our singlet even parity phase shifts with YLAM has been attained only through the introduction of V_{LL} . It has been known for some time that the local central potential, adjusted to fit the zero

TABLE 4 (b)
Triplet odd parity nuclear bar phase shifts for coupled partial waves

E (MeV)	${}^3\theta P_1$	${}^3\theta P_2$	ρ_2	${}^3\theta P_4$	${}^3\theta H_4$	ρ_4	${}^3\theta H_6$	${}^3\theta K_4$	ρ_6
10	0.010	0.000	-0.007						
20	0.029	0.001	-0.021						
40	0.073	0.005	-0.048	0.001	0.000	-0.005			
60	0.118	0.009	-0.069	0.002	0.001	-0.009			
80	0.161	0.013	-0.082	0.003	0.002	-0.015			
100	0.198	0.017	-0.090	0.005	0.002	-0.019	0.001	0.000	-0.004
120	0.229	0.020	-0.094	0.008	0.003	-0.024	0.001	0.001	-0.006
140	0.255	0.022	-0.095	0.011	0.004	-0.028	0.001	0.001	-0.008
160	0.275	0.024	-0.094	0.015	0.006	-0.032	0.001	0.001	-0.009
180	0.290	0.025	-0.092	0.020	0.007	-0.036	0.001	0.001	-0.011
200	0.301	0.026	-0.088	0.025	0.008	-0.039	0.001	0.002	-0.012
220	0.309	0.025	-0.084	0.031	0.009	-0.043	0.002	0.002	-0.014
240	0.314	0.025	-0.080	0.038	0.010	-0.045	0.002	0.003	-0.016
260	0.315	0.023	-0.075	0.046	0.011	-0.048	0.002	0.003	-0.017
280	0.315	0.021	-0.070	0.055	0.012	-0.050	0.003	0.003	-0.019
300	0.312	0.019	-0.065	0.064	0.013	-0.052	0.003	0.004	-0.020
320	0.308	0.016	-0.062	0.075	0.014	-0.053	0.004	0.004	-0.022

Notations are those of ref. 4)

energy scattering parameters and at the same time the $\delta(^1S_0)$ of the Berkeley solution No. 1 at 310 MeV¹³⁾, which agrees very well with YLAM, gives too large a $\delta(^1D_2)$. The discrepancy is only about 0.06 at 310 MeV, but this is sufficient to destroy the fit to the differential cross section for $\theta < 30^\circ$. Gammel and Thaler¹³⁾ have recently considered † a non-local potential model to improve the fits of $\delta(^1D_2)$ and $\delta(^1G_4)$. Our V_{LL} is very similar to their non-local model in its effect. Without the V_{LL} our central potential would give 0.079, 0.172 and 0.255 for $\delta(^1D_2)$ at 100, 200 and 300 MeV, respectively. At the same energies $\delta(^1G_4)$ would be 0.008, 0.020 and 0.032. Comparison of these values with those in table 3 shows the importance of V_{LL} in the singlet even parity state. The V_{LL} itself is very weak, but one notices the large eigenvalues of L_{12} in eq. (5).

The $\delta(^3P_0)$ of YLAM has a well-defined maximum of 0.225 at about 55 MeV. Our $\delta(^3P_0)$ reaches a somewhat broader maximum of 0.188 at the same energy. At 100 MeV our $\delta(^3P_0)$ is still lower than YLAM by 0.015, but for 120 MeV

† It has been stated by Noyes³⁾ that Gammel and Thaler's non-local model is tailored for the Berkeley No. 2 solution¹³⁾. This is incorrect. It seems to us that the $\delta(^1S_0)$ and $\delta(^1D_2)$ of No. 2 solution are extremely difficult to fit even with the non-local model.

$< E < 260$ MeV the agreement is practically complete. Our $\delta(^3P_0)$ is lower than YLAM by 0.01 at 300 MeV but this is well within the standard deviation. The $\delta(^3P_1)$, $\delta(^3F_3)$ and $\delta(^3H_5)$ are all consistently higher than YLAM values over most of the energy range concerned. For $\delta(^3P_1)$ the discrepancy is at most barely outside the standard deviation of YLAM. For $\delta(^3F_3)$ the discrepancies are 0.005, 0.009 and 0.003 at 100, 200 and 300 MeV, respectively. For $\delta(^3H_5)$ the discrepancy never exceeds 0.003. To summarize, the triplet odd parity uncoupled phase shifts in table 4(a) are in good agreement with YLAM except for $\delta(^3P_0)$ at $E < 100$ MeV.

We now turn the discussion of coupled phase shifts (table 4(b)). Our $^3\theta_2^P$ versus energy curve and that of YLAM cross at 70 MeV, with ours running above YLAM above this energy. The difference is ≈ 0.017 , 0.008, 0.011 and 0.010 at 40, 100, 200 and 300 MeV, respectively. At the same energies our $^3\theta_2^F$ is higher than YLAM by 0.0016, 0.0062, 0.016 and 0.012. The agreement in ρ_2 is complete between 140 and 220 MeV. The discrepancy at other energies is well within the standard deviation of YLAM. We may conclude that our $J = 2$ coupled phase shifts are in fair agreement with YLAM. An apparently serious disagreement is found in $^3\theta_4^F$. Our $^3\theta_4^F$ is higher than YLAM by 0.001, 0.012 and 0.032 at 100, 200 and 300 MeV, respectively. These relatively large discrepancies at higher energies appear to be responsible for somewhat unsatisfactory fits to the p-p differential cross sections at $\theta \approx 40^\circ$ for $E > 200$ MeV. We shall discuss this point later in more detail. Our $^3\theta_4^H$ is also higher than YLAM but the difference, which increases with energy, is still 0.0034 at 300 MeV. For ρ_4 there is an excellent agreement, the discrepancy being less than 0.005.

Before discussing the representation of experimental data by our model, it may be appropriate to describe briefly how the total (nuclear and Coulomb) p-p scattering matrix has been constructed from the calculated nuclear phase shifts. Let S be the total scattering matrix. The nuclear scattering matrix S_N is introduced through ¹²⁾

$$S = e^{i\Phi} S_N e^{i\Phi},$$

where Φ is a diagonal matrix with the elements Φ_L , the L -th Coulomb phase shifts [†], so that $S_C = e^{2i\Phi}$ is the Coulomb scattering matrix. The total reaction matrix R can be written as

$$R = S - 1 = e^{i\Phi} S_N e^{i\Phi} - 1 = e^{i\Phi} (S_N - 1) e^{i\Phi} + R_C,$$

where $R_C = S_C - 1$ leads to the well-known Coulomb scattering amplitude. Again neglecting the difference between the nuclear p-p and the n-p phase

[†] It suffices to calculate Φ_L relative to the S wave Coulomb phase shift Φ_0 since $e^{2i\Phi_0}$ appears as the common phase factor in all scattering amplitudes and hence does not contribute to observable quantities.

shifts, one can now construct S_N and hence R from the calculated nuclear phase shifts. Expressions for scattering amplitudes in terms of the matrix elements of R are found in ref. ¹²⁾ The same reference also contains the expressions for experimental parameters in terms of scattering amplitudes.

Representations of the p-p experimental parameters by the model are shown in figs 4 to 12. Experimental points are taken from ref. ⁴⁾ unless otherwise stated in figure captions. The impression one gets from these figures would be that one is now in the position to understand the p-p scattering *quantitatively* in terms of the potential model. We shall conclude this section with a few remarks.

We first notice in fig. 5 that the predicted $I(\theta)$ have broad humps around 40° above 200 MeV. The major cause for these humps is our too large $\delta(^3F_4)$. For example, when the $\delta(^3F_4)$ is reduced by 0.03 at 312 MeV the hump seen in fig. 5 disappears completely. The same change also improves the fit slightly in the Coulomb interference region. In terms of the potential model such a change

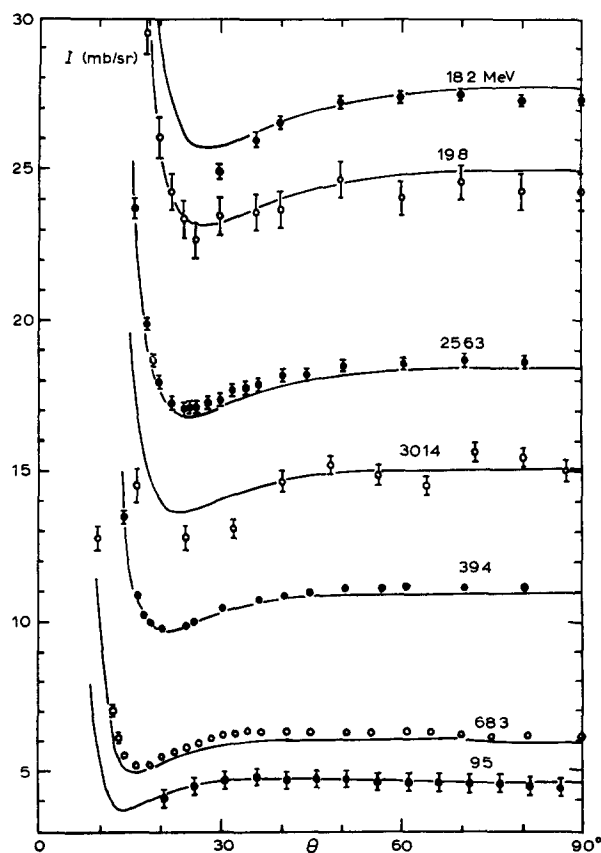


Fig. 4. The p-p differential cross sections at 18.2, 19.8, 25.63, 30.14, 39.4, 68.3 and 95 MeV. Experimental points at 30.14 MeV are taken from Hess ¹⁶⁾

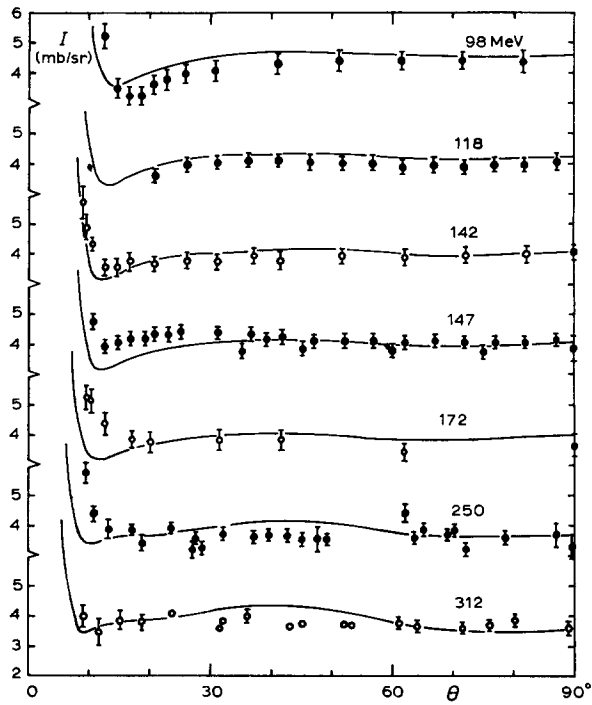


Fig 5 The p-p differential cross sections at 98, 118, 142, 147, 172, 250 and 312 MeV. Experimental points shown as at 312 MeV are taken from Chamberlain *et al* ¹⁵⁾ and ref ¹²⁾

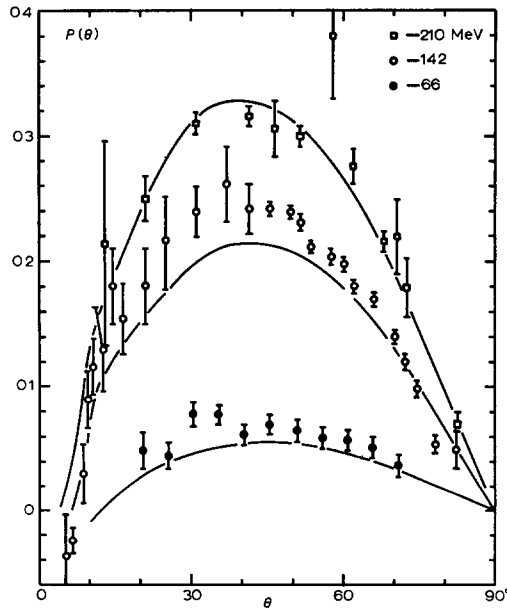


Fig 6 The p-p polarizations at 66, 142 and 210 MeV

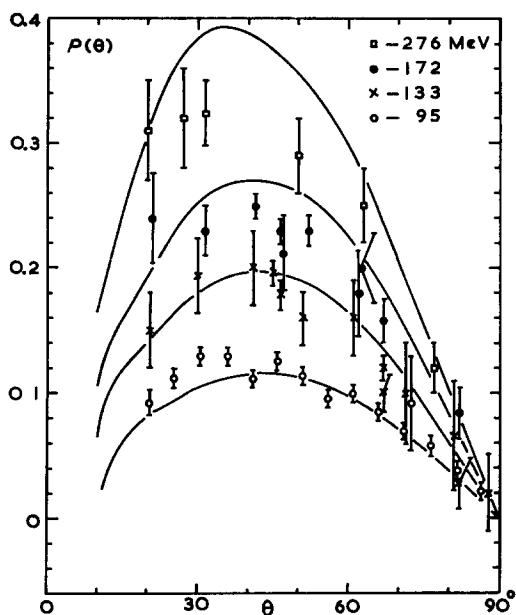


Fig 7 The p-p polarizations at 95, 133, 172 and 276 MeV

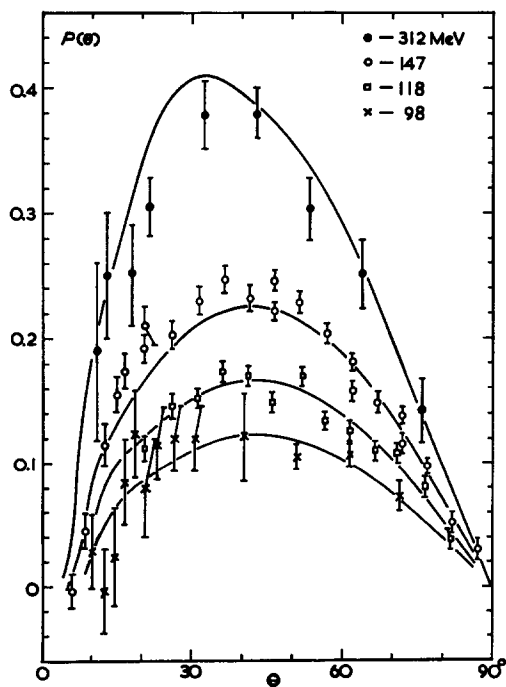


Fig 8 The p-p polarizations at 98, 118, 147 and 312 MeV

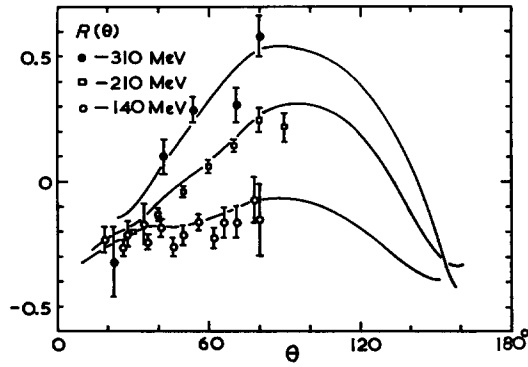


Fig 9 The p-p rotation of polarization R at 140, 210 and 310 MeV

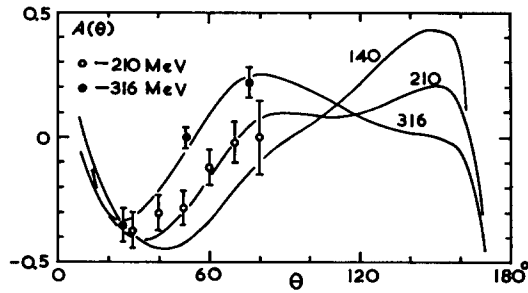


Fig 10 The p-p triple scattering parameter A at 140, 210 and 316 MeV Revised values of A at 213 MeV have been circulated by the Rochester group¹⁷⁾ The new values -0.090 ± 0.046 and -0.189 ± 0.077 at 80° and 90° , respectively, seem to be hard to fit with the phase shifts currently accepted

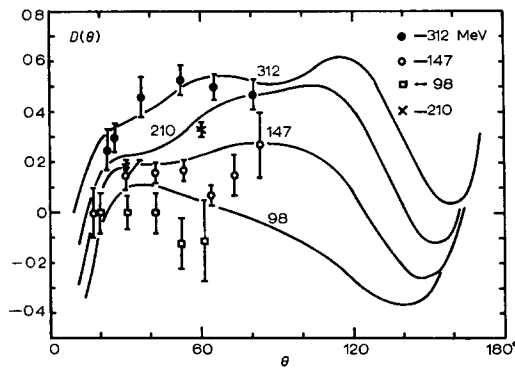


Fig 11 The p-p depolarization D at 98, 147, 210 and 312 MeV

would suggest a V_{LS} with shorter range. The objection to the shorter ranged V_{LS} comes from the polarization data $P(\theta)$ below 150 MeV, particularly at 147 and 142 MeV. As they stand, the predicted P at 20° - 50° are consistently lower than the data at these two energies (figs 6 and 8). The shorter ranged V_{LS} would mean an even smaller P at these energies. One would meet similar difficulties also at 95 and 66 MeV. The Bryan potential¹⁸⁾, which has a much shorter ranged V_{LS} than ours, indeed predicts definitely too small a P at 100 and 150 MeV.

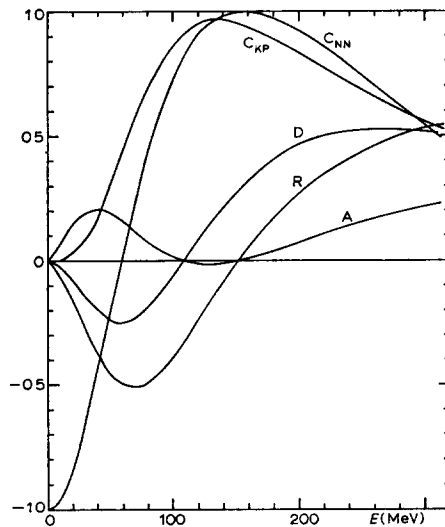


Fig 12 The p-p triple scattering and spin correlation parameters at 90° versus E

Although our calculations are admittedly limited, it does not seem possible to find a V_{LS} which meets these two conflicting demands: sufficiently long ranged so as to affect seriously the P-wave scattering below 150 MeV, but not to affect the F-wave scattering above 200 MeV. For some unknown reasons (the dynamical relativistic effect could be one of them), it appears that the V_{LS} becomes ineffective for the F and higher partial waves at high energies^{19, 20)}. To some extent this requirement may be satisfied if we add another term proportional to $(\sigma_1 \cdot \sigma_2) L^2$ to our triplet odd parity potential. The experience with the H1 potential indicates, however, that the quantitative fits to both the I above 200 MeV, and P below 150 MeV would still be difficult.

In fig 5 we see that the fits in the Coulomb interference region becomes increasingly poorer with increasing energy. The adjustment in $\delta(^3F_4)$, as described above, improves the fit slightly but does not account for the large discrepancies present at 172 and 250 MeV. Our computer programme neglects the phase shifts for $J > 6$, and we suspect that this is at least partly responsible

for the unsatisfactory representation of I in the Coulomb interference region. This point has, however, not been proved.

5. n-p Scattering

The $T = 0$ phase shifts calculated from our model are shown in tables 5 and 6(a). Again the coupled phase shifts in table 6(a) are Blatt-Biedenharn phase shifts. The same phase shifts in the bar scheme are given in table 6(b).

TABLE 5

Singlet odd parity phase shifts calculated from the potential defined by eqs (1) to (4) and table 1

E (MeV)	1P_1	1F_3	1H_5
10	-0 048	-0 001	
20	-0 080	-0 005	
40	-0 118	-0 015	-0 002
60	-0 147	-0 025	-0 004
80	-0 175	-0 033	-0 007
100	-0 205	-0 039	-0 010
120	-0 236	-0 045	-0 014
140	-0 269	-0 051	-0 016
160	-0 303	-0 056	-0 019
180	-0 336	-0 062	-0 022
200	-0 370	-0 068	-0 025
220	-0 404	-0 074	-0 027
240	-0 438	-0 081	-0 030
260	-0 472	-0 088	-0 032
280	-0 505	-0 096	-0 035
300	-0 537	-0 104	-0 037
320	-0 569	-0 113	-0 040

TABLE 6 (a)

Triplet even parity Blatt-Biedenharn phase shifts calculated from the potential defined by eqs (1) to (4) and table 1

E (MeV)	3D_2	3G_4	3I_6	3S_1	3D_1	ε_1	3D_3	3G_3	ε_3	3G_5	3I_5	ε_5
10	0 015			1 795	-0 012	0 022	0 001	-0 001	0 763			
20	0 048	0 002		1 507	-0 037	0 031	0 007	-0 007	0 760			
40	0 122	0 008	0 001	1 216	-0 091	0 040	0 020	-0 022	0 732	0 002	-0 003	0 823
60	0 192	0 018	0 002	1 015	-0 142	0 048	0 037	-0 039	0 704	0 004	-0 007	0 818
80	0 245	0 027	0 005	0 876	-0 187	0 056	0 053	-0 054	0 682	0 008	-0 011	0 813
100	0 290	0 038	0 007	0 759	-0 227	0 064	0 067	-0 067	0 661	0 011	-0 016	0 808
120	0 324	0 048	0 010	0 659	-0 263	0 073	0 081	-0 079	0 643	0 014	-0 021	0 804
140	0 352	0 058	0 013	0 579	-0 296	0 083	0 092	-0 090	0 626	0 017	-0 026	0 799
160	0 372	0 066	0 016	0 508	-0 327	0 094	0 103	-0 100	0 611	0 020	-0 032	0 795
180	0 386	0 074	0 019	0 443	-0 356	0 106	0 113	-0 109	0 598	0 023	-0 036	0 790
200	0 395	0 082	0 022	0 378	-0 382	0 119	0 123	-0 117	0 586	0 026	-0 041	0 786
220	0 401	0 089	0 025	0 322	-0 407	0 132	0 131	-0 125	0 575	0 028	-0 046	0 782
240	0 403	0 095	0 028	0 271	-0 432	0 146	0 139	-0 133	0 566	0 031	-0 051	0 779
260	0 402	0 100	0 031	0 223	-0 455	0 162	0 145	-0 140	0 557	0 033	-0 055	0 775
280	0 400	0 106	0 033	0 178	-0 477	0 177	0 152	-0 147	0 550	0 035	-0 059	0 772
300	0 397	0 110	0 036	0 136	-0 499	0 194	0 157	-0 153	0 543	0 037	-0 063	0 769
320	0 392	0 114	0 037	0 096	-0 520	0 211	0 162	-0 159	0 537	0 040	-0 067	0 766

The same phase shifts for coupled partial waves in the nuclear bar scheme are shown in table 6 (b)

TABLE 6(b)
Triplet even parity nuclear bar phase shifts for coupled partial waves

E (MeV)	${}^3\theta_1^s$	${}^3\theta_1^D$	ρ_1	${}^3\theta_3^D$	${}^3\theta_3^G$	ρ_3	${}^3\theta_5^G$	${}^3\theta_5^I$	ρ_5
10	1 795	-0 012	0 044						
20	1 507	-0 037	0 062						
40	1 216	-0 091	0 077	0 001	-0 003	0 042			
60	1 014	-0 141	0 088	0 005	-0 007	0 075	-0 002	-0 001	0 011
80	0 875	-0 186	0 098	0 011	-0 012	0 105	-0 002	-0 001	0 019
100	0 757	-0 225	0 106	0 017	-0 017	0 130	-0 003	-0 002	0 027
120	0 656	-0 260	0 116	0 024	-0 022	0 153	-0 004	-0 003	0 035
140	0 576	-0 293	0 127	0 030	-0 028	0 172	-0 005	-0 004	0 043
160	0 504	-0 323	0 139	0 037	-0 034	0 190	-0 007	-0 006	0 052
180	0 437	-0 350	0 151	0 043	-0 039	0 205	-0 007	-0 006	0 059
200	0 371	-0 375	0 162	0 050	-0 044	0 219	-0 008	-0 008	0 067
220	0 313	-0 398	0 174	0 056	-0 050	0 231	-0 009	-0 009	0 074
240	0 260	-0 421	0 186	0 062	-0 056	0 243	-0 010	-0 011	0 082
260	0 210	-0 442	0 200	0 067	-0 062	0 252	-0 010	-0 012	0 088
280	0 163	-0 462	0 211	0 072	-0 067	0 263	-0 011	-0 013	0 094
300	0 118	-0 481	0 224	0 076	-0 072	0 270	-0 011	-0 015	0 100
320	0 075	-0 499	0 237	0 080	-0 077	0 277	-0 011	-0 016	0 107

Notations are those of ref ⁵⁾

There is a reasonable agreement between the singlet odd parity phase shifts given in table 5 and those of YLAN3M⁵⁾ At lower energies our $\delta(^1P_1)$ runs below YLAN3M by less than 0 016 which is just outside the standard deviation There is a crossing at 90 MeV, and above this energy our $\delta(^1P_1)$ is higher than YLAN3M The difference is 0 01, 0 02 and 0 03 at 200, 250 and 300 MeV, respectively For $\delta(^1F_3)$ the agreement is practically complete below 200 MeV The difference above this energy is at most barely outside the standard deviation of YLAN3M

The $\delta(^3D_2)$ of YLAN3M has a broad maximum of 0 405 at about 200 MeV, while ours reaches the same maximum value at about 240 MeV. The discrepancy is, however, hardly significant in view of the large standard deviation of YLAN3M, $\approx \pm 0 04$ Below 200 MeV our $\delta(^3D_2)$ is consistently lower than YLAN3M, by as much as 0 05 at about 100 MeV The $\delta(^3G_4)$ agrees with YLAN3M to within the standard deviation $\approx \pm 0 004$

The suppression of $\delta(^3D_2)$ at higher energies as indicated by YLAN3M is exactly what was found necessary in a previous paper ²⁾ The strong negative V_T at $x \approx 1$, which seems to be required by the deuteron data, gives very large $\delta(^3D_2)$ (see eq (6)) If one puts $V_{LL} \equiv 0$ in our triplet even parity potential and adjust the hard core radius to fit the deuteron binding energy as mentioned in sect 3, the $\delta(^3D_2)$ is 0 390, 0 677 and 0 820 at 100, 200 and 300 MeV, respectively With such large $\delta(^3D_2)$ it is clearly impossible to fit the total n-p cross sections above, say, 150 MeV Comparison of $\delta(^3D_2)$ in table 6(a) and these large values will convince the reader that the central and tensor forces alone are

not adequate unless strong energy dependence of V_T is invoked. The short ranged V_{LS} cannot help much in this respect as the impact parameter considerations indicate. Indeed, any V_{LS} with the strength and range similar to ours would change $\delta(^3D_2)$ by only $\approx \pm 0.02$ even at 300 MeV. The inclusion of V_{LL} is then a natural step to take. Pion theoretical calculations do indicate the existence of such a potential^{6,7)} Although our V_{LL} itself is weak in agreement with the pion theory indications, its effect on the $\delta(^3D_2)$ is very large (reduction of 0.422 at 300 MeV) because of the large eigenvalue of L_{12} as seen in eq. (6). The reductions in $\delta(^3G_4)$ and $\delta(^3I_6)$ of 0.039 and 0.009, respectively, at 300 MeV are also appreciable.

The $^3\theta_1^S$ of table 6(b) runs above YLAN3M for $E < 250$ MeV. The discrepancy is well within the standard deviation above 200 MeV. The discrepancy increases with decreasing energy and at 20 MeV it is 0.12. For $^3\theta_1^D$ there is a good agreement below 100 MeV. Above this energy our $^3\theta_1^D$ is appreciably higher than YLAN3M, by 0.065 and 0.08 at 200 and 300 MeV, respectively. In view of very large standard deviation of YLAN3M ρ_1 , we may regard the agreement in ρ_1 satisfactory. Our $^3\theta_3^D$ runs below YLAN3M over the whole energy range. The difference increases with the energy but does not exceed 0.017, which is well within the standard deviation. For $^3\theta_3^G$ there is a very good agreement below 200 MeV. Above this energy our $^3\theta_3^G$ is higher than YLAN3M, by 0.016 and 0.043 at 250 and 300 MeV, respectively. The ρ_3 of YLAN3M reaches the maximum value of about 0.205 at 200 MeV and remains almost constant above this energy. Our ρ_3 , on the other hand, passes 0.205 at 180 MeV and keeps increasing with energy. At 300 MeV our ρ_3 is higher than YLAN3M by 0.065, which is just outside the standard deviation. A very similar situation holds for ρ_5 . YLAN3M reaches a broad maximum of 0.063 at 240 MeV while our ρ_5 increases monotonically with energy. At 300 MeV our ρ_5 is higher than YLAN3M by 0.040. Our $^3\theta_5^G$ is consistently higher than YLAN3M, but the difference is well within the standard deviation.

Representation of the n-p experimental parameters by the model are shown in figs. 13 to 16. Experimental points are taken from ref. 5). As a whole the fits are satisfactory. We conclude with two remarks. First, a slightly too high cross section for $\theta \approx 80^\circ$ at 42 MeV (fig. 13) is most certainly due to our too large $\delta(^3S_1)$. A reduction of about 0.06 (in the total of 1.18 at 42 MeV) in $\delta(^3S_1)$ would be required to make the fit satisfactory. It is an open question whether such a reduction can be attained with the potential model consistent with the deuteron data. Our experience makes us feel, however, that it would not be very easy. The second remark is concerned with the backward cross sections at higher energy. The calculated $I(180^\circ)$ tends to be too low, which is particularly the case in fig. 15. Calculations show that the backward scattering amplitude is extremely sensitive to the singlet odd parity phase shifts. As mentioned earlier our computer programme neglects entirely the phase shifts for $Jl > 6$.

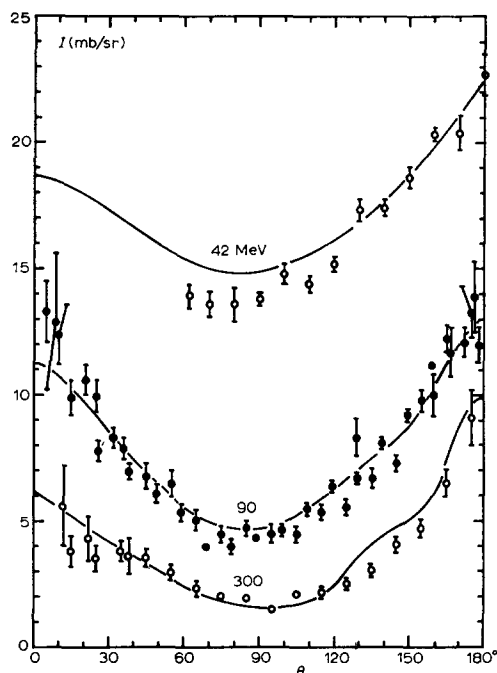


Fig. 13 The n-p differential cross sections at 42, 90 and 300 MeV

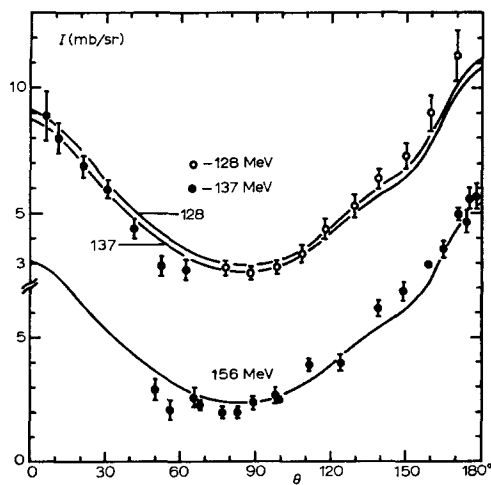


Fig. 14 The n-p differential cross sections at 128, 137 (upper scale) and 156 MeV (lower scale).

Judging from table 5 this neglect may not be quite justified. This may be, at least partly, responsible for somewhat poorer representation of the backward scattering

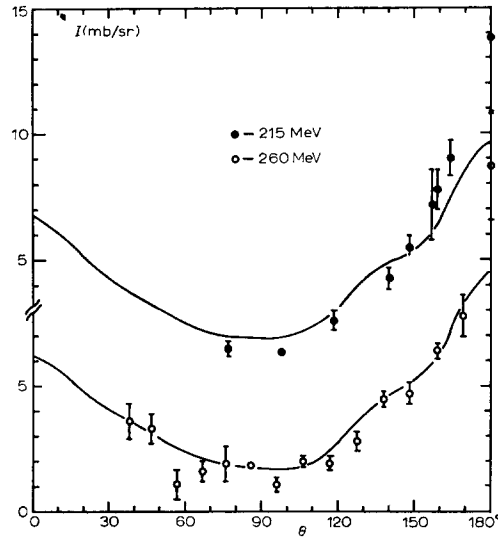


Fig 15 The n-p differential cross sections at 215 (upper scale) and 260 MeV (lower scale).

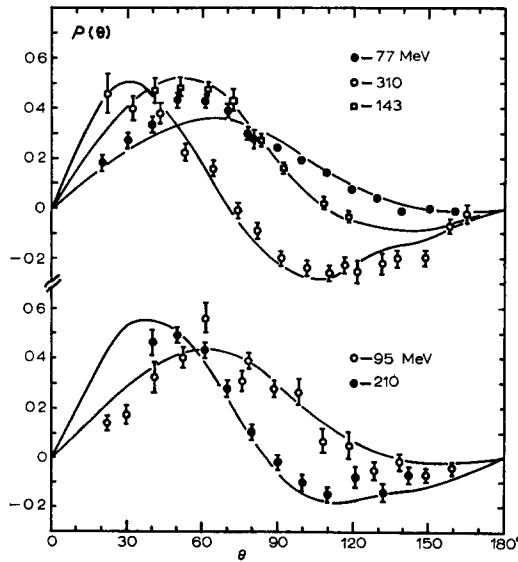


Fig 16 The n-p polarizations at 77, 95, 143, 210 and 310 MeV.

6. Conclusion

The potential model defined by eqs (1) to (4) and table 1 represents both the p-p and n-p data below 315 MeV in a satisfactory manner as shown in figs 4 to 16. Apart from the usual central and tensor parts, the model is characterized by a short ranged strong linear LS potential in the triplet odd state and a weak but long ranged quadratic LS potential in the triplet even state. The latter potential is present also in the singlet states. The phase shifts calculated from the model are in fair agreement with the Yale solutions YLAM ($T = 1$) and YLAN3M ($T = 0$).

We believe that the present model may be used in the calculations of nuclear problems other than those considered in the present paper. The model will also be useful in checking the compatibility of any potentials, derived from field theory or otherwise, with the experimental two-nucleon data.

It is a pleasure to express our sincere gratitude to Professor H A Bethe and Professor G Breit for stimulating comments and generous encouragement. To Professor Breit we are also grateful for communicating to us several unpublished numerical values of phase shifts obtained by the Yale group. We are indebted to Professor H Messel for providing excellent research facilities which have been so essential to carry out the present investigation, and to Professor S T Butler for the encouragement which has initiated our co-operation. All the numerical work reported in the present paper has been carried out on SILLIAC at the Basser Computing Department and we gratefully acknowledge generous assistance offered by the members of the Department.

References

- 1) T Hamada, Prog Theor Phys **24** (1960) 1033
- 2) T Hamada, Prog Theor Phys **25** (1961) 247
- 3) H P Noyes, in Proc 1960 Ann Int Conf on High Energy Physics at Rochester (University of Rochester, 1960) p 117
- 4) G Breit, M H Hull, K E Lassila and K D Pyatt, Phys Rev **120** (1960) 2227
- 5) M H Hull, K E Lassila, H M Ruppel, F A McDonald and G Breit, Phys Rev **122** (1961) 1606
- 6) S Okubo and R E Marshak, Ann Phys **4** (1958) 166
- 7) N Hoshizaki and S Machida, Prog Theor Phys **24** (1960) 1325
- 8) J K Perring and R J N Phillips, Nuclear Physics **23** (1961) 153
- 9) T Hamada and I D Johnston, Prog Theor Phys **26** (1961) 153
- 10) H A Bethe and P Morrison, Elementary nuclear theory, 2nd ed (John Wiley and Sons, Inc, New York, (1956) p 93
- 11) J M Blatt and L C Biedenharn, Rev Mod Phys **24**, (1952) 258
- 12) H P Stapp, T J Ypsilantis and N Metropolis, Phys Rev **105** (1957) 302
- 13) M H MacGregor, M J Moravcsik and H P Stapp, Phys Rev **116** (1959) 1284
- 14) J L Gammel and R M Thaler, in Progress in elementary particle and cosmic ray physics **V**, (North-Holland Publ Co, Amsterdam, 1960) p 99

- 15) O Chamberlain, E Segré, R D Tripp, C Wiegand and T Ypsilantis, Phys Rev **105** (1957) 288
- 16) W N Hess, Rev Mod Phys **30** (1958) 368
- 17) A C England, W A Gibson, K Gotow, E Heer and J Tinlot, University of Rochester Report NYO-9686
- 18) R A Bryan, Nuovo Cim **16** (1960) 895
- 19) G Breit, Phys Rev **111** (1958) 652
- 20) M H Hull, K D Pyatt, C R Fisher and G Breit, Phys Rev Lett **2** (1959) 264